IJPSR (2019), Volume 10, Issue 3 **(Research Article)**

INTERNATIONAL JOURNAL OF PHARMACEUTICAL SCIENCES AND RESEARCH

Received on 06 July 2018; received in revised form, 04 September 2018; accepted, 10 September 2018; published 01 March 2019

HIGHLY SELECTIVE AND SENSITIVE DETERMINATION OF Cr^{6+} (nM) IN GELATIN CAPSULE USING AgF/Ag_2WO_4 NANOCOMPOSITE

Ramya Arumugam and Prakash Periakaruppan *

Department of Chemistry, Thiagarajar College, Madurai - 625009, Tamil Nadu, India.

Keywords:

AgF/Ag_2WO_4 Nanocomposite, Colorimetric sensor, Gelatin capsule, Chromium

Correspondence to Author:
Dr. Prakash Periakaruppan

Assistant Professor,
Department of Chemistry,
Thiagarajar College, Madurai - 625009, Tamil Nadu, India.

E-mail: kmpprakash@gmail.com

ABSTRACT: The present work deals with a novel synthesis of AgF/Ag_2WO_4 nanocomposite by co-precipitation method. The morphology and size of the synthesized AgF/Ag_2WO_4 nanocomposite were confirmed by Ultraviolet-Visible (UV-Vis) spectroscopy, Fourier Transform-Infrared (FT-IR) spectroscopy, Transition Electron Microscopy (TEM) and X-Ray Diffraction (XRD) analyses. The performance of the nanocomposite was successfully evaluated for Cr^{6+} detection in a gelatin capsule, which indicated that this convenient and sensitive material offered great promise for onsite environmental monitoring of Cr^{6+}. Control experiments with the addition of over 10 other metal ions (Na^+, K^+, Mg^{2+}, Fe^{2+}, Hg^{2+}, Ca^{2+}, Cu^{2+}, Ni^{2+}, Mn^{2+}, Zn^{2+}) did not result in a distinct change in the colour or in the spectrum of the suspension which indicated that these ions did not interfere in the colorimetric determination of Cr^{6+} in gelatin capsule. The detection concentration of Cr (VI) ranged from 0.5 mg to 1.0 mg, and the detection limit was 2 nM.

INTRODUCTION: High soluble and toxic content with the carcinogenic effect of hexavalent chromium Cr^{6+} has been consistently found to be associated with an elevated incidence of respiratory cancers and other adverse health consequences. Chromium commonly exists in nature with two stable oxidation states, Cr^{3+} and Cr^{6+}, whereas Cr^{6+} is highly water soluble and toxic, Cr (III) is much less soluble in water and less toxic to humans in the absence of complexing ligands [1-3]. Many industries produce this carcinogenic pollutant including leather tanning, cement, textile, printers and stainless steel welding [4-7].

QUICK RESPONSE CODE

DOI: 10.13040/IJPSR.0975-8232.10(3).1439-47

The article can be accessed online on www.ijpsr.com

DOI link: http://dx.doi.org/10.13040/IJPSR.0975-8232.10(3).1439-47

There are several methods used for the detection of Cr^{6+} such as atomic emission spectrometry, atomic absorption spectrometry, electrochemical method, and UV-vis spectrophotometry, X-ray fluorescence, solid phase extraction and solvent extraction [8-15].

Among all the above-said methods, they are considered as a simple and low-cost, fast and portable and easy to carried out. Such a cost-effective monitoring tool for the detection of Cr^{6+} in gelatin capsule is of essential relevance, particularly in sensitive environments like pharmaceuticals, groundwater and industrial wastewater effluents. For the last few decades, pharmaceutical products have been growing rapidly in the global market. This development is highly expected to a greater extent because of the growth of a huge population and efficient health treatments [16-21]. Generally, gelatin capsules are administered to heal. The chromium content has been checked in various medicines such as Cipmox 250, OMEGA

B-Complex capsule, N-Cycline-250 and Doxylab. Among them, the chromium content is particularly more in N-Cycline-250 medicinal capsule. Many research literature has reported the evaluation of drug composition in pharmaceuticals, but no work has been carried out for the detection of a trace amount of chromium in empty gelatin capsules.

In the last few decades, the nanomaterials have been significant due to their various physical and chemical properties. Due to fascinating electronic, optical, magnetic, chemical and biological properties, the bimetallic nanomaterials exhibit new bifunctional or synergic effects [22-23]. One of the transition metal compounds, tungstates possess a combination of covalent, ionic and metallic bonding and form an essential class of functional materials. Tungstates render important properties like ferroelectricity, conductivity, and photo-luminescence which have attracted significant attention among the scientific community due to its unique symmetry dependent and spontaneous polarization properties [24-26].

Among the tungstates, silver tungstate is emerging as a new material which shows high potential applications in enormous fields such as sanitary ceramics as an antibacterial agent, plasmonics, high-temperature tribological applications as solid-state lubricants, the catalyst for water splitting and dye degradation, electrochemical sensor, antibacterial property, luminescence host [27-35,] *etc*. Various methods are involved during the preparation of tungsten oxides such as sol-gel method, chemical precipitation method and microwave irradiation method [36-38]. Among them, chemical precipitation method plays a vital role due to its simple operation, less consumption of time and purity of the material compared to other methods. Ag and F is the best candidate as a dopant for Ag_2WO_4. AgF nanoparticles were formed due to the diffusion of Ag^+ which reacted with the adsorbed F^-. These nanoparticles are low cost, stable and nontoxic.

The present work, reports the synthesis of novel AgF/Ag_2WO_4 nanocomposite. The synthesized nanocomposite has been characterized by UV-visible spectroscopy, FT-IR spectroscopy, XRD, HR-TEM, and EDX analyze. To the best of our knowledge, this is the first ever reported study which probes a highly selective and sensitive detection of Cr^{6+} in gelatin capsule using AgF/Ag_2WO_4 nanocomposite.

Experimental: All the reagents used in this work were analytical grade and used without further purification. All chemicals such as silver nitrate, sodium fluoride and sodium tungstate ($Na_2WO_4.2H_2O$) were purchased from Sigma Aldrich, India. The commercial gelatin capsules were purchased from Apollo Pharmacy, Madurai, India. Deionized water (DI) was used throughout the work.

Preparation of AgF: 10 mmol $AgNO_3$ and 2.5 mmol NaF were each separately dissolved in 20 ml of DI water. NaF solution was stirred constantly for 10 min and then added dropwise to $AgNO_3$ solution with constant stirring for 3 h and there obtained a light grey colored suspension, which was centrifuged to remove the precipitate by washing twice with water and ethanol and dried in an oven at 333 K for 24 h.

Preparation of Ag_2WO_4: The Ag2WO4 was prepared by a precipitation process at room temperature. In a typical procedure, 0.5 mM of Na_2WO_4 was dissolved in 20 ml of DI water to form a clear solution, followed by a dropwise addition of 20 ml of $AgNO_3$ aqueous solution (0.025 M). The solution turned white, indicating the formation of Ag_2WO_4. The precipitate formed was continuously stirred for 1 h and collected by centrifugation. After washing the as-prepared Ag_2WO_4 three times with DI water and ethanol, it was dried at 60 °C for 6 h.

Preparation of AgF/Ag_2WO_4 Nanocomposite: In an experimental procedure, 0.023 g of the as-prepared Ag_2WO_4 was added into 15 mL of DI water with the assistance of ultrasonication. 0.023g of prepared AgF was added into Ag_2WO_4 solution. After continuously stirred for 2 h at room temperature in the dark, the products were collected by centrifugation.

The obtained products were washed with DI water and ethanol three times each and dried at 60 °C for 6 h. **Scheme 1** illustrates the formation of the AgF/Ag_2WO_4 nanocomposite and its sensing of Cr^{6+} in gelatin capsules.

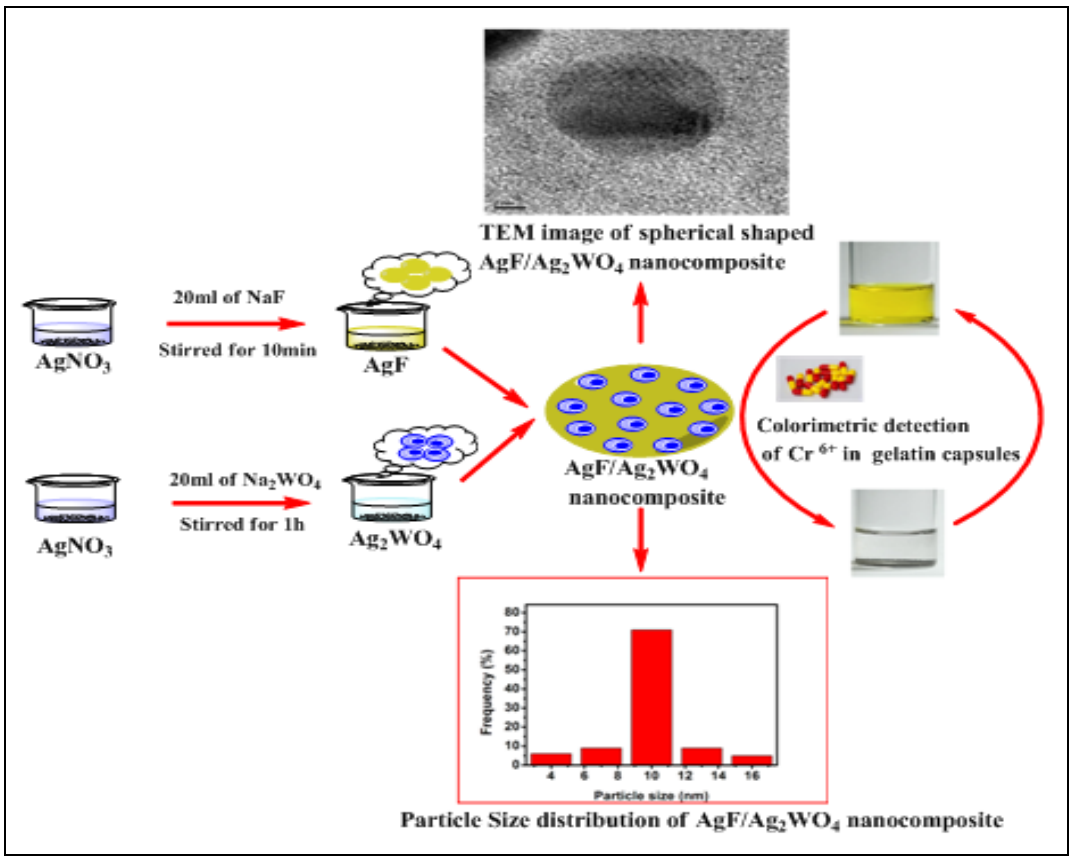

SCHEME 1: SYNTHESIS OF AgF/Ag_2WO_4 NANOCOMPOSITE AND ITS SENSING PROPERTIES OF Cr^{6+} IN GELATIN CAPSULE

Instrumentation: UV-visible spectra (Jasco V-560 model) of synthesized AgF/Ag_2WO_4 nano-composite was recorded between the range 200-800nm. The FT-IR spectral measurement was recorded using a KBr disc on a JASCO FT-IR 460 Plus spectrophotometer which was collected at a spatial resolution of 4 cm^{-1} in the transmission mode between 4000-400 cm^{-1}. XRD analysis was carried out using an X-ray diffraction unit using Cu Ka radiation (λ = 1.5418Aº) on a JEOL JDX 8030 X-ray diffract meter. The size and morphology of synthesized AgF/Ag_2WO_4 nanocomposite were examined using transmission electron microscopy (HR-TEM, JEOL JEM 2100 model) instruments. An Energy Dispersive X-ray (EDX) spectrometer was used for elemental analysis which was attached to the transmission electron microscope. All experiments were carried out at room temperature.

RESULTS AND DISCUSSION:

UV-Vis Spectroscopy: The UV–vis spectra of the samples AgF, Ag_2WO_4 and AgF/Ag_2WO_4 are depicted in **Fig. 1.** The UV-vis absorption spectrum of AgF sample exhibits a peak at 427 nm with absorption in the visible region. The spectrum for Ag_2WO_4 sample has an absorption maximum at 420 nm. The peak at 422 nm confirms the formation of AgF/Ag_2WO_4 nanocomposite [39].

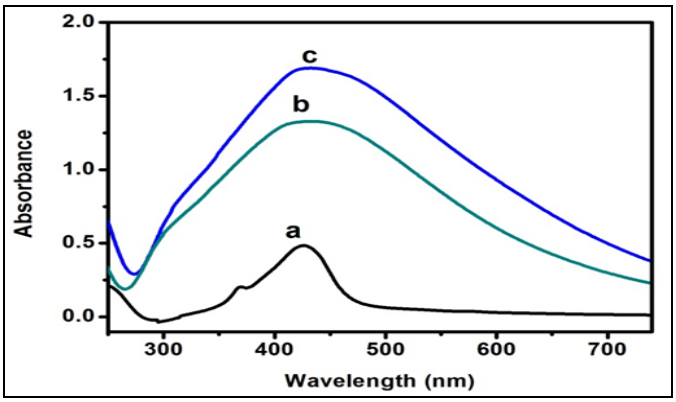

FIG. 1: UV-VISIBLE SPECTRA OF SYNTHESIZED AgF (A), Ag_2WO_4 (B) AND AgF/Ag_2WO_4 (C) NANOCOMPOSITE

FT-IR Spectroscopy: Fig. 2 shows the FT-IR spectra of AgF, Ag_2WO_4, and AgF/Ag_2WO_4 nanocomposite. In both the samples Ag_2WO_4 and AgF/Ag_2WO_4, FT-IR spectra show the absorption band at 3399 cm^{-1} and 1350 cm^{-1} which indicates that the presence of -OH stretching and its corresponding H-OH vibration appears at 1650 cm^{-1}. The peak appears at 2300 cm^{-1} assigned C-H

stretching vibration. The strong vibrational peak appears at 856 cm^{-1} for both the samples Ag_2WO_4 and AgF/Ag_2WO_4 which is ascribed to asymmetric stretching vibrations of the O-W-O indicates the characteristic of tetrahedral tungstate [40]. Although a broad absorption peak appears at 746-825 cm^{-1} for the synthesized AgF/Ag_2WO_4 nanocomposite which can also be observed due to the existence of WO_4^{2-} anions [41].

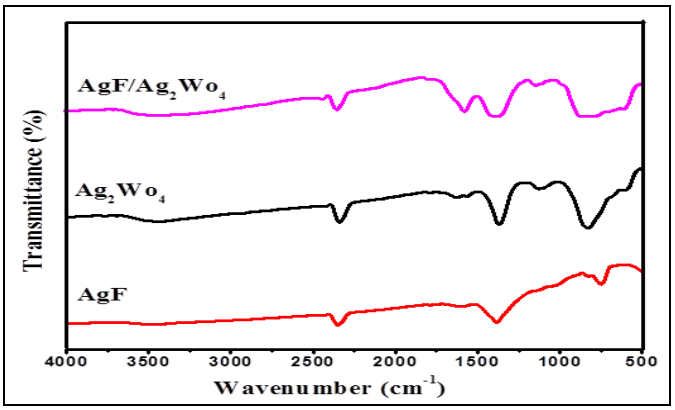

FIG. 2: FT-IR SPECTRUM OF AgF, Ag_2WO_4, AgF/Ag_2WO_4 NANOCOMPOSITE

XRD Measurement: Fig. 3 explains the diffraction peaks for the crystalline structure of as-prepared AgF/Ag_2WO_4 nanocomposite with the corresponding 2θ values and crystal planes. The diffraction peaks of AgF sample (JCPDS No 3-890) denote the crystalline structure of AgF/Ag_2WO_4. The characteristics peaks of AgF at 29.2°, 38.9°, 56.1°, 70.3° are gradually observed and well matched with the (111), (200), (220), (222) plane of the face-centered cubic structure. The main characteristic peaks of Ag_2WO_4 at 13.9°,15.7°, 16.7°, 19.5°, 26.7°, 32.9°, 33.8°, 37.4°, and 40.8° can be indexed to the (020), (121), (022), (220), (200), (040), (242), (060) and (224), crystal planes of Ag_2WO_4 (JCPDS 34-0061) with orthorhombic phase. The extra peaks on composite particles compared to AgF at 2θ values of 31.7°, 45.4° and 56.4° corresponding to the crystal planes (111), (200) and (220) indicate the presence of Ag metal (JCPDS card no.04-0783) [42]. Furthermore, the diffraction peak of the AgF/ Ag_2WO_4 has been shifted to a small degree compared to AgF which indicates that there is an effective interaction between AgF and Ag_2WO_4 in AgF/Ag_2WO_4 nanocomposite. The size of the synthesized AgF/Ag_2WO_4 nanocomposite was calculated using Debye Scherrer's equation and found to be 10 nm.

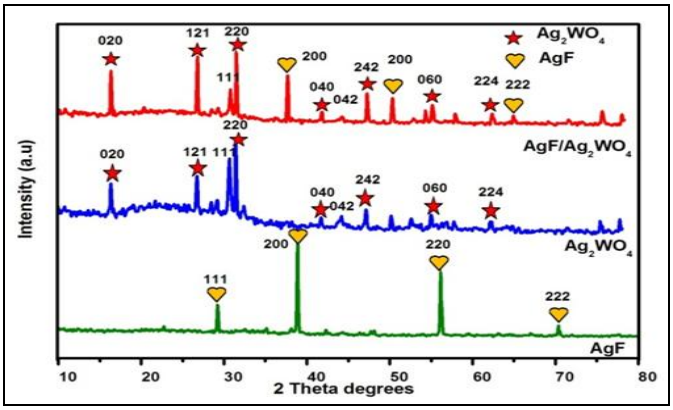

FIG. 3: XRD MEASUREMENT OF AgF, Ag_2WO_4, AgF/Ag_2WO_4 NANOCOMPOSITE

TEM: The surface morphology, size, and shape of the AgF/Ag_2WO_4 nanocomposite were characterized by HR-TEM images.

Fig. 4(a-d) displays the HR-TEM images with different magnifications of the synthesized AgF/Ag_2WO_4 nanocomposite. **Fig. 5(a)** presents the selected-area electron diffraction (SAED) patterns which describes the concentric diffraction bright spots corresponding to the presence of (020), (121), (111), (220), (200), (242), (200) and (222) planes of the face-centered cubic (fcc) AgF/ Ag_2WO_4 nanocomposite. The EDX spectrum as shown in **Fig. 5b** for the AgF/Ag_2WO_4 nanocomposite indicates the presence of major elements such as Ag, F, W, and O. **Fig. 5(c)** shows the histogram analysis for finding the average size of synthesized AgF/Ag_2WO_4 nanocomposite and found to be 10 nm which agrees well with the size confirmed using Sherrer's equation.

Colorimetric Sensing of Cr^{6+} in Gelatin Capsules using AgF/Ag_2WO_4 Nanocomposite Selectivity Studies: The synthesized AgF/Ag_2WO_4 nanocomposite was tested for the detection of Cr^{6+} in gelatin capsules over other environmental metal cations by adding different heavy metal cations such as Na^+, K^+, Mg^{2+}, Fe^{2+}, Hg^{2+}, Ca^{2+}, Cu^{2+}, Ni^{2+}, Mn^{2+} and Zn^{2+} to the AgF/Ag_2WO_4 nanocomposite solution and color changes were recorded.

Fig. 6 represents the photographic image of AgF/Ag_2WO_4 nanocomposite with different heavy metal cations. There is no change in color observed when other heavy metal ions were added to the composite solution except for Cr^{6+} in gelatin capsule solution.

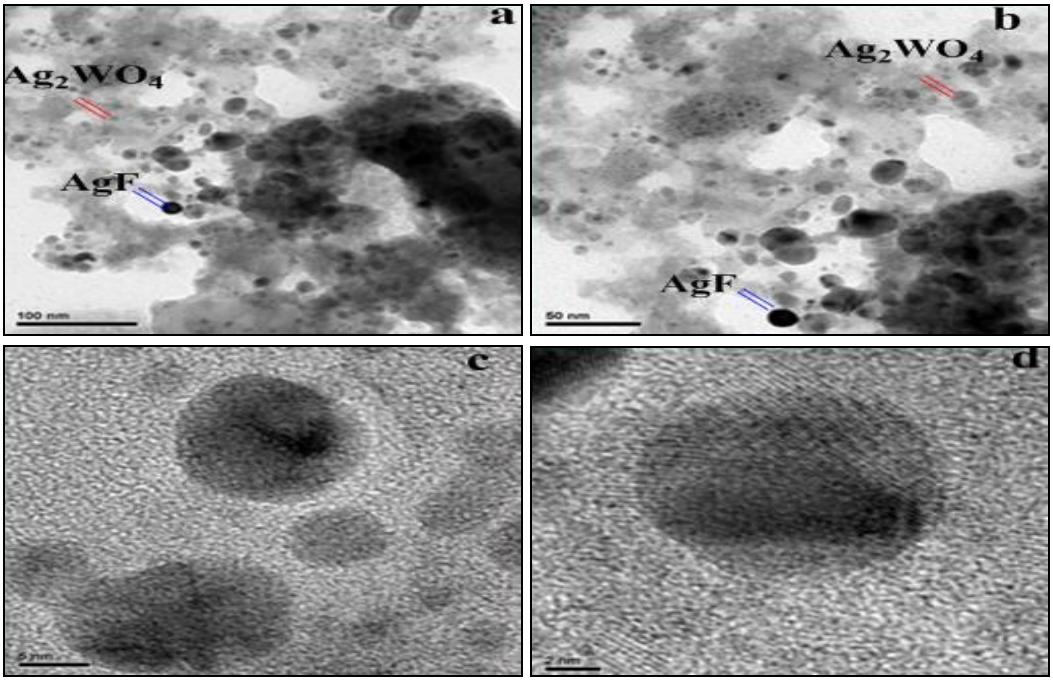

FIG. 4 (A-D): TEM IMAGES OF DIFFERENT MAGNIFICATIONS OF AgF/Ag_2WO_4 NANOCOMPOSITE

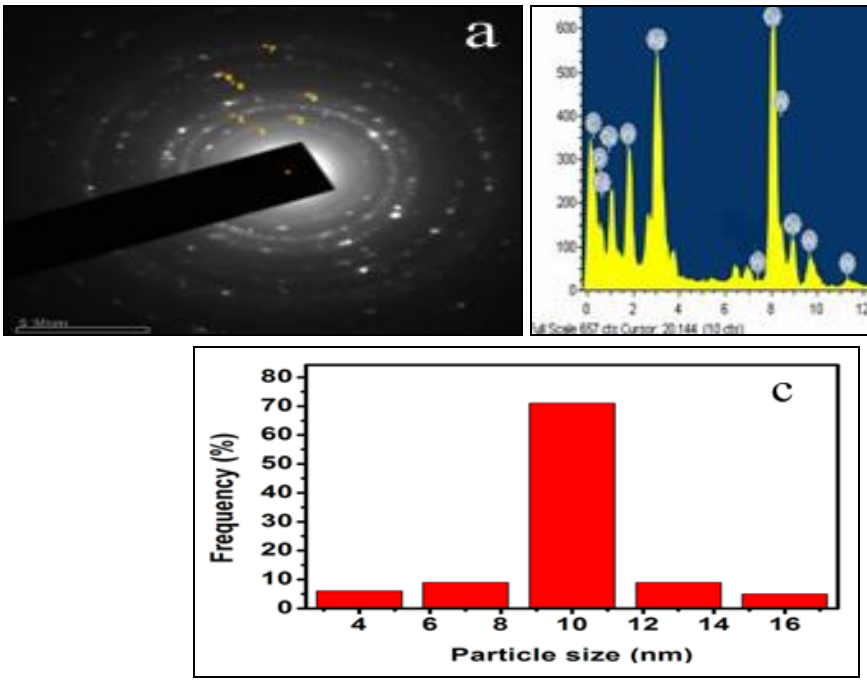

FIG. 5: (A) SAED PATTERN OF AgF/Ag_2WO_4 NANOCOMPOSITE (B) EDX SPECTRUM OF AgF/Ag_2WO_4 NANOCOMPOSITE (C) HISTOGRAM OF PARTICLE SIZE DISTRIBUTION OF AgF/Ag_2WO_4 NANOCOMPOSITE

Adding different heavy metal cations to AgF/Ag_2WO_4 nanocomposite has been recorded by UV-vis absorption spectra that were shown in **Fig. 7(a).** A few differences in selectivity histogram of AgF/Ag_2WO_4 nanocomposite for Cr^{6+} in gelatin capsule are shown in **Fig. 7(b).**

It shows that the change in the absorption peak is high selectivity. It is confirmed from the selectivity results that the proposed colorimetric sensor can detect specifically Cr^{6+} in a gelatin capsule.

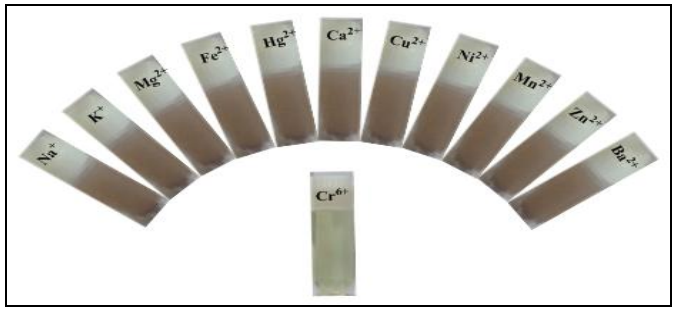

FIG. 6: PHOTOGRAPHIC IMAGE OF AgF/Ag_2WO_4 NANOCOMPOSITE WITHIN DIFFERENT HEAVY METAL CATIONS

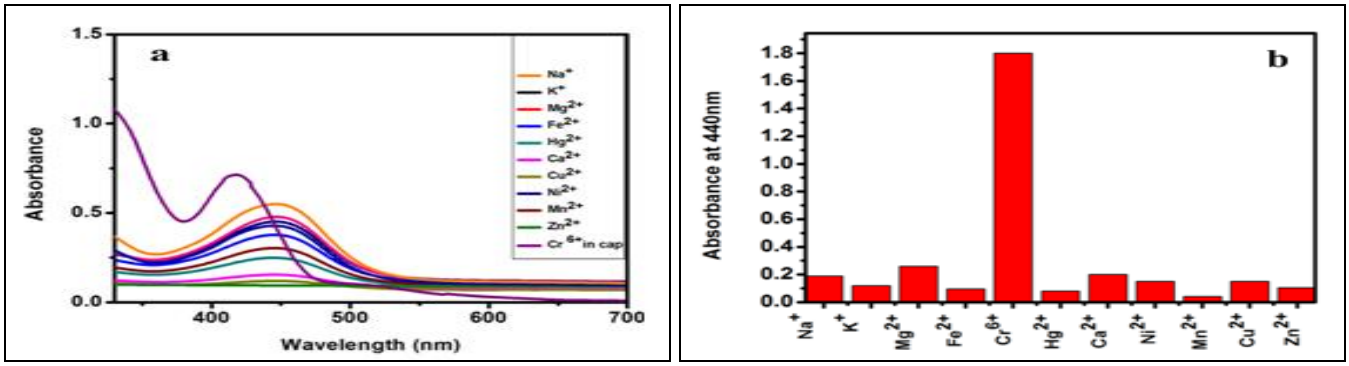

FIG. 7: (A) UV-VISIBLE SPECTRA OF AgF/Ag_2WO_4 NANOCOMPOSITE SOLUTION WITH DIFFERENT TRANSITION-METAL IONS. (B) THE COLORIMETRIC RESPONSE OF AgF/Ag_2WO_4 NANOCOMPOSITE TO VARIOUS METAL CATIONS

Sensitivity Studies: To detect the sensing range of this sensor, sensitivity studies were carried out. For these investigations, the prepared solution of 1mM of AgF/Ag_2WO_4 nanocomposite was diluted with distilled water. Then, 1.5 mL of AgF/Ag_2WO_4 nanocomposite was mixed with 1 mL of various amounts (0.5 mg - 1.0 mg) of Cr^{6+} in gelatin capsule solution. When Cr^{6+} in gelatin capsule solution is added to AgF/Ag_2WO_4 nano-composite, a significant color change is observed from yellow to colorless. The color changes are observed due to the redox reaction between silver and chromium. The photographic image of AgF/Ag_2WO_4 nanocomposite in the presence of a different quantity of Cr^{6+} in gelatin capsule solution was depicted in **Fig. 8.**

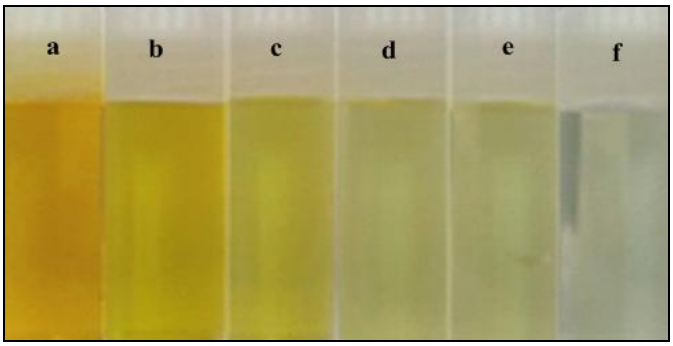

FIG. 8(A-F): PHOTOGRAPHIC IMAGES OF AgF/Ag_2WO_4 NANOCOMPOSITE WITH VARIOUS QUANTITIES (0.5 mg - 1.0 mg) OF Cr^{6+} IN GELATIN CAPSULE

Further, it was proved by using UV-vis spectroscopy by measuring the SPR intensity of AgF/Ag_2WO_4 nanocomposite. The UV-vis spectra of AgF/Ag_2WO_4 nanocomposite in the presence of different concentrations of Cr^{6+} are seen from **Fig. 9(a).** The absorbance intensity of AgF/Ag_2WO_4 nanocomposite gradually decreases while increasing the concentration of Cr^{6+} from 0.5 mg - 1.0 mg.

The absorbance values of AgF/Ag_2WO_4 nano-composite versus the concentration of Cr^{6+} was plotted and shown in **Fig. 9(b)**. It shows a linear relationship (R^2 = 0.9988) between the SPR absorbance of AgF/Ag_2WO_4 nanocomposite at 441 nm and Cr^{6+} at concentration from 0.5 mg to 1.0 mg. The lowest limit of detection can be calculated as:

$$LOD = 3S/b$$

Where S is the standard deviation of the lowest concentration of Cr^{6+} and b is the slope of the calibration curve. The synthesized AgF/Ag_2WO_4 nanocomposite is found to sense Cr^{6+} with the limit of detection (LOD) of 2 nM. The HR-TEM images obtained for AgF/Ag_2WO_4 nanocomposite before and after the addition of Cr^{6+} in gelatin capsule are shown in **Fig. 10**. As seen, while well-defined AgF/Ag_2WO_4 nanocomposite appears before addition **Fig. 10a**, it disappears after the addition of Cr^{6+} in gelatin capsule **Fig. 10b**. **Fig. 10c** presents the elemental analysis of the AgF/Ag_2WO_4 nanocomposite using EDX which confirms the existence of Ag, W, and O. **Fig. 10d** confirms the existence of Ag, W, O, and Cr after sensing Cr^{6+} in the gelatin capsule. The sensitivity of this colorimetric sensor has been compared to those of earlier studies using nanoparticles sensors as shown in **Table 1** which shows a superior limit of detection for the proposed sensor [43-47].

Real Sample Analysis: An application of AgF/Ag_2WO_4 as a colorimetric sensor in the analysis of gelatin capsule spiked with Cr^{6+} was made. The detected concentration of Cr^{6+} was 2 nM, close to that of the added Cr^{6+} (0.5 - 1.0 mg). The recovery was 84%. These results indicate that AgF/Ag_2WO_4 has good accuracy in monitoring Cr^{6+} in gelatin capsules.

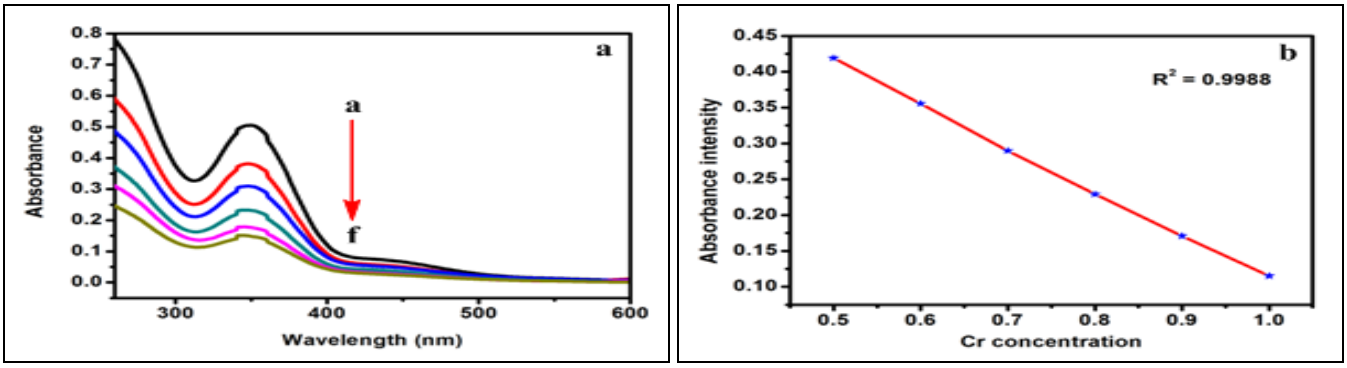

FIG. 9: A) UV-VISIBLE ABSORPTION SPECTRA OF AgF/Ag_2WO_4 NANOCOMPOSITE AFTER THE ADDITION OF VARIOUS QUANTITIES (0.5 mg - 1.0 mg) of Cr^{6+} IN GELATIN CAPSULE (A-F) B) PLOT OF ABSORBANCE INTENSITY VERSUS Cr

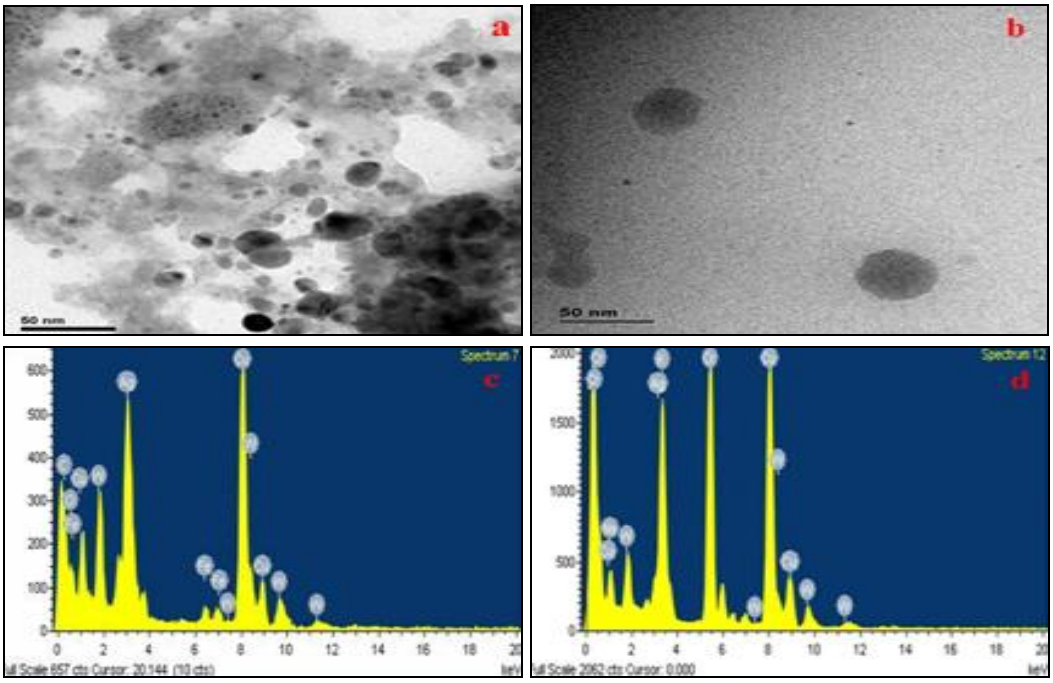

FIG. 10: TEM IMAGE OF AgF/Ag_2WO_4 NANOCOMPOSITE BEFORE (A) AND AFTER (B) ADDITION OF Cr IN GELATIN CAPSULE AND EDX SPECTRA OF AgF/Ag_2WO_4 NANOCOMPOSITE BEFORE (C) AND AFTER (D) ADDING Cr IN GELATIN CAPSULE

TABLE 1: COMPARISON OF COLORIMETRIC SENSORS PROPOSED FOR DETECTION OF Cr^{6+} IN THE LITERATURE

Materials	Size	Shape	Linearity coefficient (R^2)	Linear range	LOD	References
AgNPs	-	-	0.993	1×10^{-6} to 5×10^{-5} M	4.5×10^{-7} M	43
AuNPs	17nm	-	0.9975	100–600 nM	20 nM	44
AgNPs	10-20nm	Spherical	0.956	500-5000 ppm	0.441×10^{-6} M	45
AgNPs	50-60 nm	Spherical	0.9852	100 mM- 1 µM	1 µM	46
BSA-Au NPs/STCP	14.06 ± 3.14 nm	-	0.9928	0.5 µM -50.0 µM	280 nM	47
AgF/Ag_2WO_4	10nm	Spherical	0.9988	0.5 mg - 1.0 mg	2 nM	Present work

CONCLUSION: In summary, we have reported here a facile and novel synthesis of AgF/Ag_2WO_4 nanocomposite. The synthesized AgF/Ag_2WO_4 nanocomposite has been employed as a simple, environmentally friendly and low-cost colorimetric sensor for the detection of Cr^{6+} in gelatin capsules. The proposed sensor shows high sensitivity, with a significant change in the color of the solution from yellow to colorless in the presence of a small amount of Cr^{6+} in gelatin capsules. There is no obvious interference from other heavy metal ions, and therefore the sensor is highly selective for Cr $^{6+}$ in gelatin capsules. The reported probe has the lowest detection limit (2 nM).

ACKNOWLEDGEMENT: The authors thank the management of Thiagarajar College for providing lab facilities.

CONFLICT OF INTEREST: There is no conflict of interest.

REFERENCES:

1. Balakumar V and Prakash P: A Facile, One-pot and Eco-friendly Synthesis of Gold/Silver Nanobimetallics Smartened RGO for Enhanced Catalytic Reduction of Hexavalent Chromium. RSC adv 2016; 6: 57380-57388.
2. Wu X, Xu Y, Dong Y, Jiang X and Zhu N: Colorimetric determination of hexavalent chromium with ascorbic acid capped silver nanoparticles. Anal. Methods 2013; 5: 560-565.
3. Ray RR: Adverse hematological effects of hexavalent chromium: an overview. Interdiscip Toxicol 2016; 9(2): 55-65.
4. Li S, Tang L, Zeng G, Wang J, Deng Y, Wang J, Xie Z and Zhou Y: Catalytic reduction of hexavalent chromium by a novel nitrogen-functionalized magnetic ordered mesoporous carbon doped with Pd nanoparticles. Env Sci and Pollution. Res 2016; 23: 22027-22036.
5. Shouqiang W, Jinqiu L, Long L, Jing S and Zhongcai S: Photocatalytic effect of iron corrosion products on reduction of hexavalent chromium by organic acids. J. Taiwan Ins Che Eng 2014; 45: 2659-2663.
6. Yadav M and Xu Q: Catalytic chromium reduction using formic acid and metal nanoparticles immobilized in a metal-organic framework. Chem Commun 2013; 49: 3327.
7. Lai YJ and Tseng WL: Role of 5-thio-(2-nitrobenzoic acid)-capped gold nanoparticles in the sensing of chromium (VI): remover and sensor. Analyst 2011; 136: 2712-2717.
8. Liu Y, Meng X, Han J, Liu Z, Meng M, Wang Y, Chen R and Tian S: Speciation, adsorption and determination of chromium(III) and chromium(VI) on a mesoporous surface imprinted polymer adsorbent by combining inductively coupled plasma atomic emission spectrometry and UV spectrophotometry. J Sep Sci 2013; 36: 3949-3957.
9. Ramajyothi N, Farook MNA, Cho M and Shim J: Analysis and Speciation of Chromium in Environmental Matrices by Various Analytical Techniques. Asian J Chem 2013; 25: 4125-4136.
10. Prakash A, Chandra S and Bahadur D: Structural, magnetic, and textural properties of iron oxide-reduced graphene oxide hybrids and their use for the electrochemical detection of chromium. Carbon 2012; 50: 4209-4219.
11. Durairaj S, Sidhureddy B, Cirone J and Chen A: Nanomaterials-based electrochemical sensors for *in-vitro* and *in-vivo.* Analyses of Neurotransmitters, Appl Scie 2018; 8: 1504-1531.
12. Kefa KO and Salomey AS: Determination of hexavalent chromium (Cr(VI)) concentrations *via* ion chromatography and UV-Vis spectrophotometry in samples collected from nacogdoches wastewater treatment plant, East Texas (USA). Adv Env Che 2016; Article ID 3468635, 1-9.
13. Tsuyumoto I and Maruyama Y: X-ray Fluorescence analysis of hexavalent chromium using K beta satellite peak observed as the counterpart of X-ray absorption near-edge structure pre-edge peak. Anal. Chem 2011; 83(19): 7566-7569.
14. Ma J, Yang B and Byrne RH: Determination of nanomolar chromate in drinking water with solid phase extraction and a portable spectrophotometer. J Hazar Mater 2012; 219-220: 247-52.
15. Tadayon F and Abadi HFR: Speciation of chromium in organic fruit samples with cloud point extraction separation and preconcentration and determination by UV-Vis spectrophotometry. Aca. Res International 2014; 5(2): 140-147.
16. The-Telegraph. Chinese police arrest 22 over toxic drug capsules.http://www.telegraph.co.uk/news/worldnews/asia/china/9208216/Chinese-police-arrest-22-over-toxic-drug-capsules.html, 2012.
17. Xinhua. Toxic capsules reignite concerns over drug safety. http://www.chinadaily.com.cn/business/2012/04/17/content 15070215.htm, 2012.
18. Xinhua. 22 nabbed for producing toxic drug capsules. http://www.china.org.cn/china/2012/04/17/content_25161446.htm, 2012.
19. Welling R, Beaumont JJ, Petersen SJ, Alexeeff GV and Steinmaus C: Chromium VI and stomach cancer: a meta-analysis of the current epidemiological evidence. Occup Environ Med 2015; 72: 151-159.
20. Burkitt L: China halts sale of some drugs. The Walls Street Journal. http://www.wsj.com/articles/ SB10001424052702304299304577347563418936068.
21. Goncalves DA, Gu J, Dos Santos MC, Jones BT and Donati GL: Direct determination of chromium in empty medicine capsules by tungsten coil atomic emission spectrometry. J Anal At Spectrom 2015; 30: 1395-1399.
22. Harshulkhan MS, Janaki K, Velraj G, Ganapthy SR and Nagarajan M: Effect of Ag doping on structural, optical and photocatalytic activity of tungsten oxide (WO_3) nanoparticles. J Mater Sci Mater Electron 2016; 27: 4744-4751.
23. Talapin DV, Lee JS, Kovalenko MV and Shevchenko EV: Prospects of colloidal nanocrystals for electronic and optoelectronic applications. Chem Rev 2010; 110: 389-458.
24. Joy JJJ: Doping effect an optical band gap and luminescence of pure and Nd-doped $coWO_4$ wolframite nanostructure synthesized by chemical precipitation. Inter. J Che Concepts 2015; 1(2): 44-56 .
25. Andre's J, Gracia L, Gonzalez-Navarrete P, Longo VM, Avansi W, Volanti DP, Ferrer MM, Lemos PS, La Porta FA, Hernandes AC and Longo E: Structural and electronic analysis of the atomic scale nucleation of Ag on a-Ag2WO4 induced by electron irradiation. Sci Rep 2014; 4: 5391-5397.
26. Modi D, Srinivas M, Tawde D, Murthy KVR, Verma V and Patel N: Hydrothermal synthesis and photoluminescence properties of cerium-doped cadmium tungstate nanophosphor. J Exper. Nanosci 2014; 10: 777-786.
27. Wang Q, Guo X, Wu W and Liu S: Preparation of fine Ag_2WO_4 antibacterial powders and its application in the sanitary ceramics. Adv Mater Res 2011; 284-286: 1321-1325.
28. Longo E, Cavalcante LS, Volanti DP, Gouveia AF, Longo VM, Varela JA, Orlandi MO and Andre´s J: Direct *in-situ* observation of the electron-driven synthesis of Ag filaments on α-Ag_2WO_4 crystals. Sci Rep 2013; 3: 1676-1679.
29. Stone D, Liu J, Singh DP, Muratore C, Voevodin AA, Mishra S, Rebholz C, Geb Q and Aouadi SM: Layered atomic structures of double oxides for low shear strength at high temperatures. Scripta. Mater 2010; 62: 735-738.

30. Lin Z, Li J, Zheng Z, Yan J, Liu P, Wang C and Yang GW: Electronic Reconstruction of α-Ag_2WO_4 Nanorods for Visible-Light Photocatalysis. ACS Nano 2015; 9: 7256-7265.
31. Wang X, Fu C, Wang P, Yu H and Yu J: Hierarchically porous metastable β-Ag_2WO_4 hollow nanospheres: controlled synthesis and high photocatalytic activity. Nanotechnology 2013; 24: 165602-165609.
32. Muthamizh S, Giribabu K, Suresh R, Manigandan R, Munusamy S, Kumar PS and Narayanan V: Silver tungstate nanoparticles: Characterization and electrochemical sensing property. Int J Chem Tech Res 2014; 6: 3392-3394.
33. Shen J, Lu Y, Liu JK and Yang XH: Design and preparation of easily recycled Ag_2WO_4@ZnO@Fe_3O_4 ternary nanocomposites and their highly efficient degradation of antibiotics. J Mater Sci 2016; 51: 7793-7802.
34. Roca RA, Sczancoski JC, Nogueira IC, Fabbro MT, Alves HC, Gracia L, Santos LPS, De Sousa CP, Andres J, Luz Jr GE, Longo E and Cavalcante LS: Facet-dependent photocatalytic and antibacterial properties of α-Ag_2WO_4 crystals: Combining Experimental Data and Theoretical Insights. Catal Sci Technol 2015; 5: 4091-4107.
35. Cavalcante LS, Almeida MAP, Avansi W, Jr, Tranquilin RL, Longo E, Batista NC, Mastelaro VR and SiuLi M: Cluster coordination and photoluminescence properties of α- Ag_2WO_4 microcrystals. Inorg Chem 2012; 51: 10675-10687.
36. Kharade RR, Mali SS, Patil SP, Patil KR, Gang MG, Patil PS, Kim JH and Bhosale PN: Enhanced electrochromic coloration in Ag nanoparticle decorated WO_3 thin films. Electrochim Acta 2013; 102: 358-368.
37. He H, Xue S, Wu Z, Yu C, Yang K, Peng G, Zhou W and Li D: Sonochemical fabrication, characterization and enhanced photocatalytic performance of Ag_2S/Ag_2WO_4 composite micro rods. Chine J of Cat 2016; 37: 1841-1850.
38. Mohammed Harshulkhan S, Janaki K, Velraj G, Ganapthy SR and Nagarajan M: Effect of Ag doping on structural, optical and photocatalytic activity of tungsten oxide (WO_3) nanoparticles. J Mater Sci: Mater Electron 2016; 27: 4744-4751.
39. Pirhashemi M and Habibi-Yangjeh A: Ultrasonic-assisted preparation of plasmonic ZnO/Ag/Ag2WO4 nano-composites with high visible-light photocatalytic performance for degradation of organic pollutants. J Colloid and Inter Sci 2017; 491: 216-229.
40. Harshulkhan MS, Janaki K, Velraj G, Ganapthy SR and Nagarajan M: Effect of Ag doping on structural, optical and photocatalytic activity of tungsten oxide (WO_3) nanoparticles. J Mater Sci Mater Electron 2016; 27: 4744-4751.
41. Roca RA, Gouveia AF, Lemosv, Gracia L, Andres J and Longo E: Formation of Ag Nanoparticles on β-Ag_2WO_4 through Electron Beam Irradiation: A Synergetic Computational and Experimental Study. Inorg Chem 2016; 55: 8661-8671.
42. Ravichandran K, Sathish P, Snega S, Karthika K, Rajkumar PV, Subha K and Sakthivel B: Improving the antibacterial efficiency of ZnO nanopowders through simultaneous anionic (F) and cationic (Ag) doping. Pow Tech 2015; 274: 250-257.
43. Sharif T, Niaz A, Najeeb M, Zaman MI, Ihsan M and Sirajuddin: Isonicotinic acid hydrazide-based silver nanoparticles as a simple colorimetric sensor for the detection of Cr^{3+}. Sensors and Actuators B 2015; 216: 402-408.
44. Tan F, Liu X, Quan X, Chen J, Li X and Zhao H: Selective detection of nanomolar Cr(VI) in aqueous solution based on 1,4-dithiothreitol functionalized gold nanoparticles. Anal Methods 2011; 3: 343-347.
45. Elavarasi M, Rajeshwari A, Alex SA, Nanda Kumar D, Chandrasekaran N and Mukherjee A: Simple colorimetric sensor for Cr(III) and Cr(VI) speciation using silver nanoparticles as a probe. Anal. Methods 2014; 6: 5161-5167.
46. Balavigneswaran CK, SujinJebaKumar T, Packiaraj MR and Prakash S: Rapid detection of Cr(VI) by AgNPs probe produced by *Anacardium occidentale* fresh leaf extracts. Appl Nanosci 2014; 4: 367-368.
47. Guo JF, Huo D, Yang M, Hou CJ, Li J, Fa H, Luo H and Yang P: Colorimetric detection of Cr (VI) based on the leaching of gold nanoparticles using a paper-based sensor. Talanta 2016; 161: 819-825.

How to cite this article:
Arumugam R and Periakaruppan P: Highly selective and sensitive determination of Cr^{6+} (nM) in gelatin capsule using AgF/Ag_2WO_4 nanocomposite. Int J Pharm Sci & Res 2019; 10(3): 1439-47. doi: 10.13040/IJPSR.0975-8232.10(3).1439-47.

All © 2013 are reserved by International Journal of Pharmaceutical Sciences and Research. This Journal licensed under a Creative Commons Attribution-NonCommercial-ShareAlike 3.0 Unported License.

This article can be downloaded to **Android OS** based mobile. Scan QR Code using Code/Bar Scanner from your mobile. (Scanners are available on Google Play store)